Autofocusing of migrated data

Jos van Trier and Fabio Rocca

ABSTRACT

Seismic data, migrated with an incorrect velocity model, show residual diffraction hyperbolas or smiles. We use a statistical estimation theory to determine residual velocities from these events and show an example to illustrate the method.

INTRODUCTION

The observation that velocity information can be obtained from diffraction events has been made by several authors (e.g. Mehta (1977), Harlan et al. (1984) and De Vries and Berkhout (1984)). Their approach to focusing migrated data has been to calculate some focusing measure (entropy) for a range of migration velocities and then to determine the correct velocity from this sampled entropy function by either trial and error or optimization methods.

Here we present a method that directly gives an estimate of the residual velocity from the migrated data, though the estimate is scaled by an unknown constant. Still, it can be used as a direction in a search algorithm that will focus the migrated data automatically.

Migration is supposed to give an image of the reflectivities. The output of migration with an incorrect velocity model, the unfocused image, can be treated as a convolution of the reflectivities with a small wavelet. We try to estimate the residual velocity from this wavelet using statistical estimation theory, where we approximate the conditional distribution of the data by a form that is a linear function of the wavelet. Furthermore, we assume that the statistical properties of the reflectivities can be modeled by a Gaussian mixture.

RESIDUAL VELOCITY ESTIMATION

In this section we will show that data, migrated with a wrong velocity, can be written as a convolution of the reflectivities with a residual wavelet. The shape of the residual wavelet is determined by the residual velocity: a smile for overmigrated data, and a hyperbola for undermigrated data.

By considering the amplitude of the residual wavelet to be small compared to the unit operator, we will be able to apply an estimation theory similar to the one described by Kostov and Rocca (1986). The focusing of the migrated data is done in a iterative fashion: we find an estimate for the residual velocity, update the velocity model and repeat the procedure.

We will derive the equations for a constant reference velocity. As the described residual modeling is based on phase shift modeling, a depth variable background velocity is easily incorporated. Even for a general velocity field the method will still work; it only needs to be put in a different framework. For example, Rothman et al. (1985) implemented residual migration based on finite difference and Kirchhoff methods.

In any case, the estimated *residual* velocity can be both space and depth variable.

Convolutional model for residual migration

Rocca and Salvador (1982) showed that small errors in the velocity model may be corrected by applying a residual migration to previously migrated data, rather than remigrating the original data with a corrected velocity field. Analogously, the image $m(x, \tau)$, that is obtained by migrating data with some (wrong) migration velocity v_M, can be constructed by residual modeling (the transpose of residual migration) with residual velocity v_ϵ:

$$v_\epsilon^2 = v^2 - v_M^2 = 2\bar{v}\Delta v, \tag{1}$$

where v is the "true" half velocity. In practice, we set $\bar{v}$ equal to the known migration velocity v_M. Using phase shift modeling, we get for $M(k_x, \omega)$, the Fourier transform of the unfocused image $m(x, t = \tau)$[1]:

$$M(k_x, \omega) = \int \exp(-ik_\tau \tau)\ R(k_x, \tau)\ d\tau, \tag{2}$$

where:

$$k_\tau = \omega\sqrt{1 - \frac{2\bar{v}\Delta v k_x^2}{\omega^2}},$$

and $R(k_x, \tau)$ is the Fourier domain representation of the reflectivities $r(x, \tau)$.

To be able to apply first order statistical estimation theory, let us consider the following:

$$M(k_x, \omega) = \int \exp\left(-i\omega\tau\sqrt{1 - \frac{2\bar{v}\Delta v k_x^2}{\omega^2}}\right)\ R(k_x, \tau)\ d\tau \tag{3}$$

[1]Residual modeling maps from the (x, τ)-domain to a domain with the same dimensions: (x, τ). To avoid confusion in equation (2) we take t (Fourier dual: ω) as the pseudo-depth variable for the unfocused image, whereas τ (dual: k_τ) denotes pseudo-depth for the focused image. In consequent equations we drop this distinction and take ω to be the Fourier dual of τ.

$$\simeq \int \exp(-\frac{i\bar{v}\Delta v k_x^2 \tau}{\omega}) \exp(-i\omega\tau) \; R(k_x,\tau) \; d\tau \tag{4}$$

$$\simeq \int (1-\frac{i\bar{v}\Delta v k_x^2 \tau}{\omega}) \exp(-i\omega\tau) \; R(k_x,\tau) \; d\tau. \tag{5}$$

Note that the approximation to the dispersion relation in equation (4) is the same as in 15 degree migration. The second approximation is a first order Taylor expansion of the exponential and is only justified when the velocity perturbations are small. One of the later sections will describe in detail the implications of this approximation.

Equation (5) is a spatial convolution over x:

$$M(x,\omega) = \int FT^{-1}_{over\ x} \; (1-\frac{i\bar{v}\Delta v k_x^2 \tau}{\omega}) \; * \; r(x,\tau) \; \exp(-i\omega\tau) \; d\tau \tag{6}$$

$$= \int \Big(\delta(x) + \Delta v \; b(x,\omega,\tau)\Big) \; * \; r(x,\tau) \; \exp(-i\omega\tau) \; d\tau, \tag{7}$$

with:

$$b(x,\omega,\tau) = -\frac{i\bar{v}\tau}{\omega} \; FT^{-1}(k_x^2), \tag{8}$$

where $FT^{-1}(k_x^2)$, the inverse Fourier transform of k_x^2, is the second derivative wavelet (e.g. $(\,1,-2,\,1)$). We can now use (first order) statistical estimation theory to get an estimate of the velocity anomaly Δv (see appendix).

We have chosen to express the model in terms of one unknown parameter Δv. It is also possible to leave the complete second derivative wavelet as an unknown. The estimation procedure then gives the residual migration operator that "best" focuses the data and this approach can be considered as an alternative to the one proposed by Dellinger and Mora (1986).

Estimation of residual velocity

In the appendix it is shown that the conditional mean estimate of the velocity anomaly is:

$$\widehat{\Delta v}(\tau) \;=\; \overline{\Delta v^2} \;\; \gamma\Big(m(x,\tau)\Big) \;\cdot\; \int \; -\Big(b(x,\omega,\tau) * m(x,\tau)\Big) \; \exp(i\omega\tau) \; d\omega, \tag{9}$$

where γ is the gradient function (see figure 1) and $\overline{\Delta v^2}$ the variance of Δv. The dot product is taken over the x-axis.

The estimation procedure thus consists of three steps.

1. The unfocused image $m(x,\tau)$ is clipped at some amplitude by the gradient operator, resulting in a section $m_{grad}(x,\tau) = \gamma\Big(m(x,\tau)\Big)$. The clip value should be chosen such that the residual wavelets are retained and the features that are uninteresting for the velocity estimation (like flat beds) are deleted. The success of the method depends of course on the separability of these two kinds of events (see also Harlan et al. (1984)).

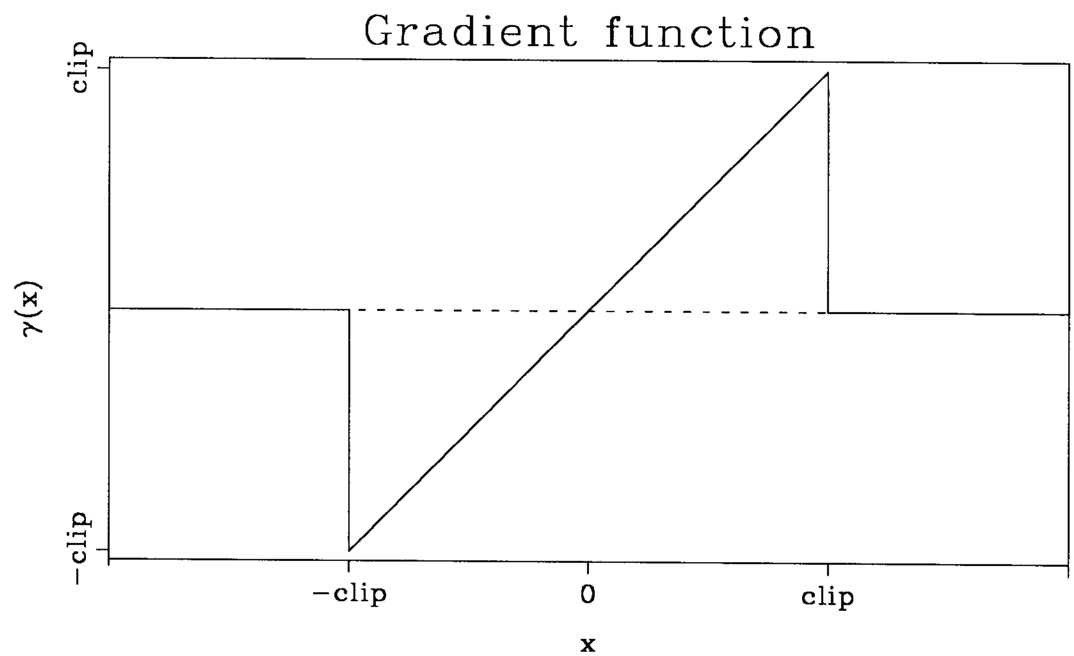

FIG. 1. The gradient function γ. We copy the figure from Godfrey (1979) (p. 39, figure 2.2d) with a slight change: Godfrey's figure displays $x - \gamma(x)$, this figure represents only $\gamma(x)$.

2. We apply the "differential" operator to the unfocused image, resulting in a section $m_{diff}(x, \tau)$:
$$m_{diff}(x,\tau) = \int -\Big(b(x,\omega,\tau) * m(x,\tau)\Big) \ \exp(i\omega\tau)\ d\omega, \tag{10}$$
or, in the Fourier domain:
$$M_{diff}(k_x,\tau) = \int \frac{i\bar{v}k_x^2\tau}{\omega} M(k_x,\omega)\ \exp(i\omega\tau)\ d\omega. \tag{11}$$

3. For each τ level, the dot product of $m_{grad}(x,\tau)$ and $m_{diff}(x,\tau)$ is taken over the x-axis, resulting in an estimate for the velocity anomaly, $\widehat{\Delta v}(\tau)$, scaled by an unknown $\overline{\Delta v^2}$. We can also take the dot product in a moving window over the x-direction, thus estimating a space variable $\widehat{\Delta v}(x,\tau)$.

As mentioned above, the estimated velocity perturbation is only known within a constant scale factor. We therefore have to use the estimate as a direction in an iterative scheme to find the final focused image.

Limits on residual velocity

The theory is based on the first order Taylor expansion of the model (see equation (5)). This

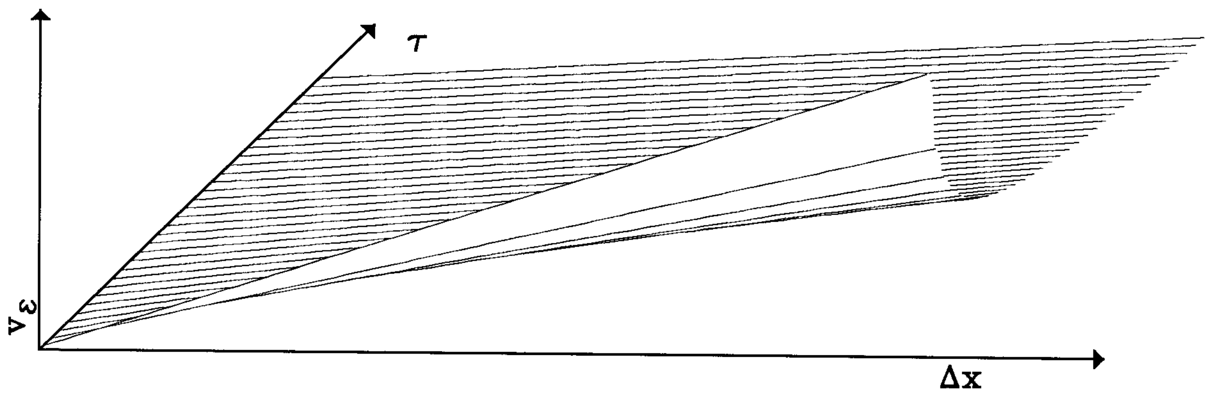

FIG. 2. The maximum value of the residual velocity as a function of Δx and τ, for fixed frequency and a given "accuracy" constant α.

approximation poses restrictions on the residual velocity; for large residual velocities the argument of the exponential in equation (4) no longer satisfies:

$$\frac{iv_\epsilon^2 k_x^2 \tau}{2\omega} < \pi^2 \frac{iv_\epsilon^2 \tau}{2\omega \Delta x^2} \ll 1, \qquad (12)$$

where we have substituted for k_x its maximum value: $\frac{\pi}{\Delta x}$, with Δx the sample interval in the x-direction. If we want the approximation to be valid within a certain accuracy range, then the left hand side of the above equation has to be smaller than some appropriate small constant α (we include π^2 in this constant):

$$\frac{iv_\epsilon^2 \tau}{2\omega \Delta x^2} < \alpha. \qquad (13)$$

Figure 2 shows the maximum value of v_ϵ as a function of Δx and τ for fixed frequency and a given α. We note that this value decreases with increasing τ and decreasing Δx. This behavior can be expected when we realize that the residual wavelet gets larger for increasing τ and decreasing Δx and that the theory is based on the wavelet being small.

Figures 3a and 3b display the same function but now for fixed Δx and two different frequency values. α has been chosen such that the first order approximation is accurate within 10 % of the exact case.

For $\Delta x = 0.01$ km and τ between 0 and 2 s, the values of the maximum residual velocities range from about 0.02 to 0.1 km/s for a frequency of 10 Hz, and from about 0.05 to 0.2 km/s for 60 Hz. These values seem to be small (especially when we consider Δv and not v_ϵ: Δv has to be smaller than 5 and 20 m/s for 10 and 60 Hz, respectively (assuming $\bar{v} = 1$ km/s)) but, as

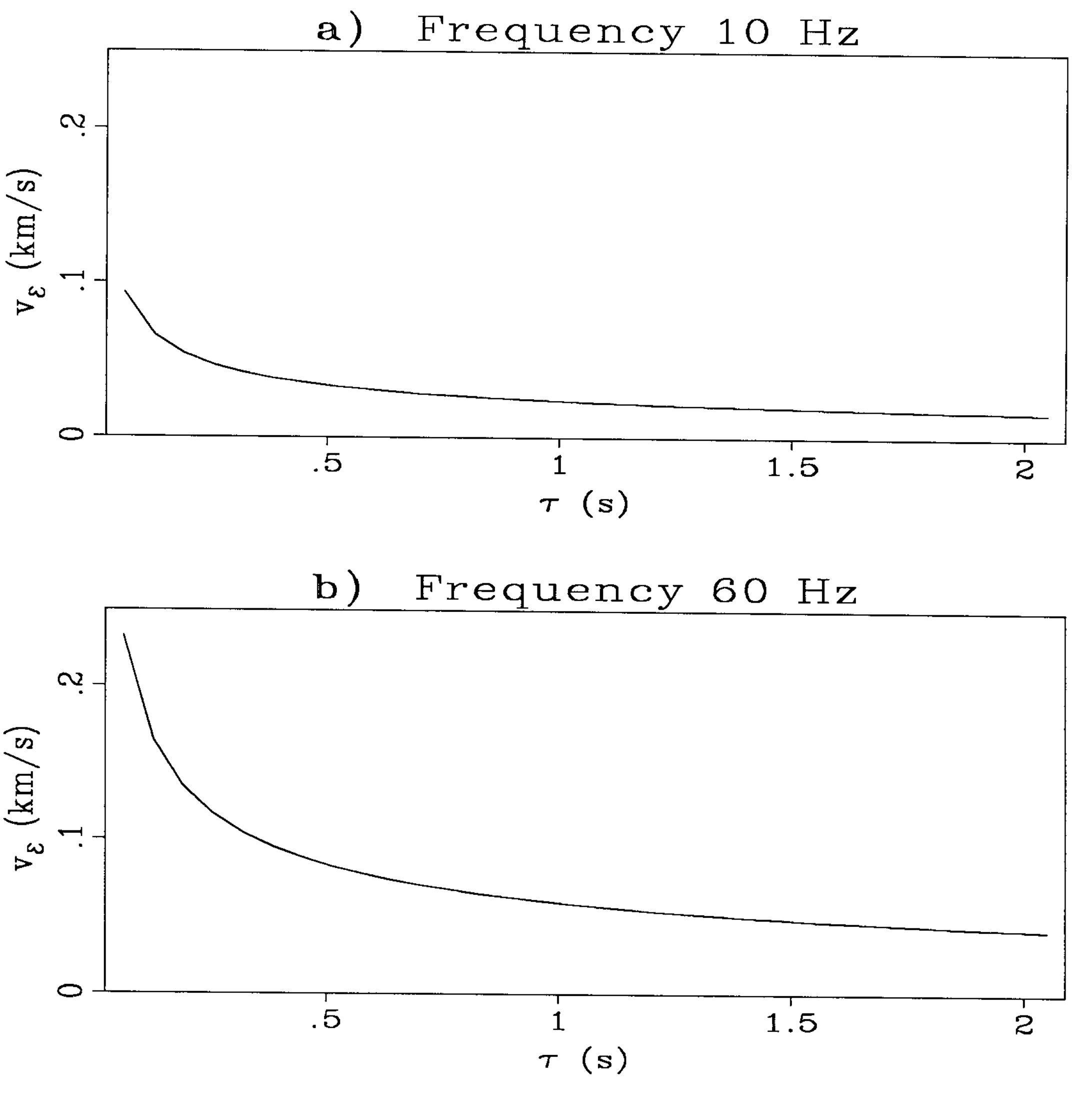

FIG. 3. The maximum residual velocity corresponding to 10 % accuracy for $\Delta x = 0.01$ km and frequencies of 10 Hz (figure a) and 60 Hz (figure b).

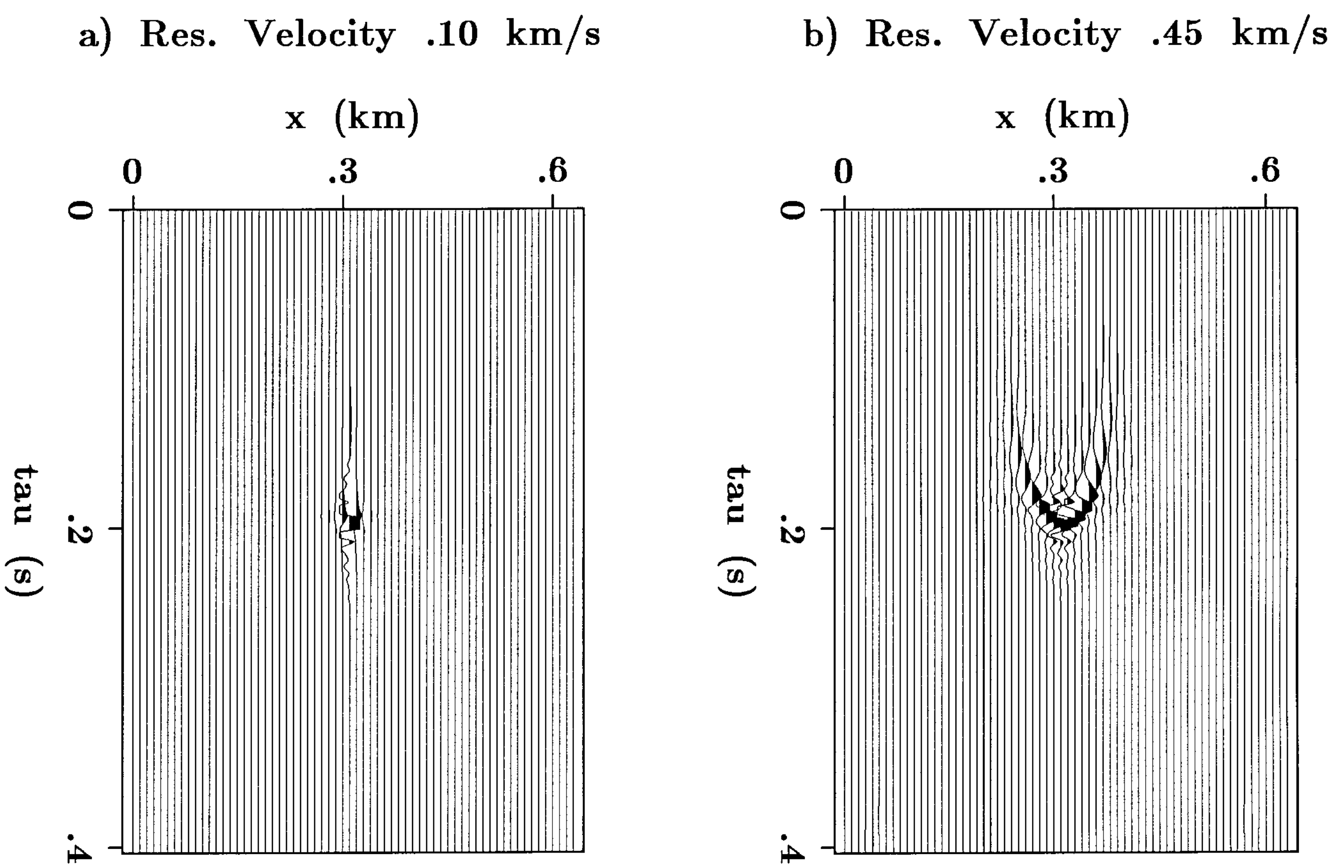

FIG. 4. unfocused images of an diffraction event; figure a shows an image that has almost been focused ($v_\epsilon = 0.10$ km/s); the spike in figure b is far from being focused ($v_\epsilon = 0.45$ km/s). The images have been plotted with the same plotting parameters.

we will see in the next section, even for larger velocity perturbations the estimation method still gives valuable information. Also, since for higher frequencies a larger residual velocity is allowed, we can high pass the data in the first iterations.

AN EXAMPLE

To illustrate the method, we generated two unfocused images of a spike function of amplitude 1, one with a residual velocity within the 10 %-accuracy region described above, and another with a much larger residual velocity (see figures 4a and 4b). In this example Δx is .01 km, $\bar{v}$ 1 km/s and the high pass cutoff frequency is 10 Hz.

We then go through each of the three steps mentioned before: figure 5 shows the clipped images $m_{grad}(x, \tau)$ (clip is 0.2), figure 6 displays $m_{diff}(x, \tau)$ and in figure 7 the estimates of the

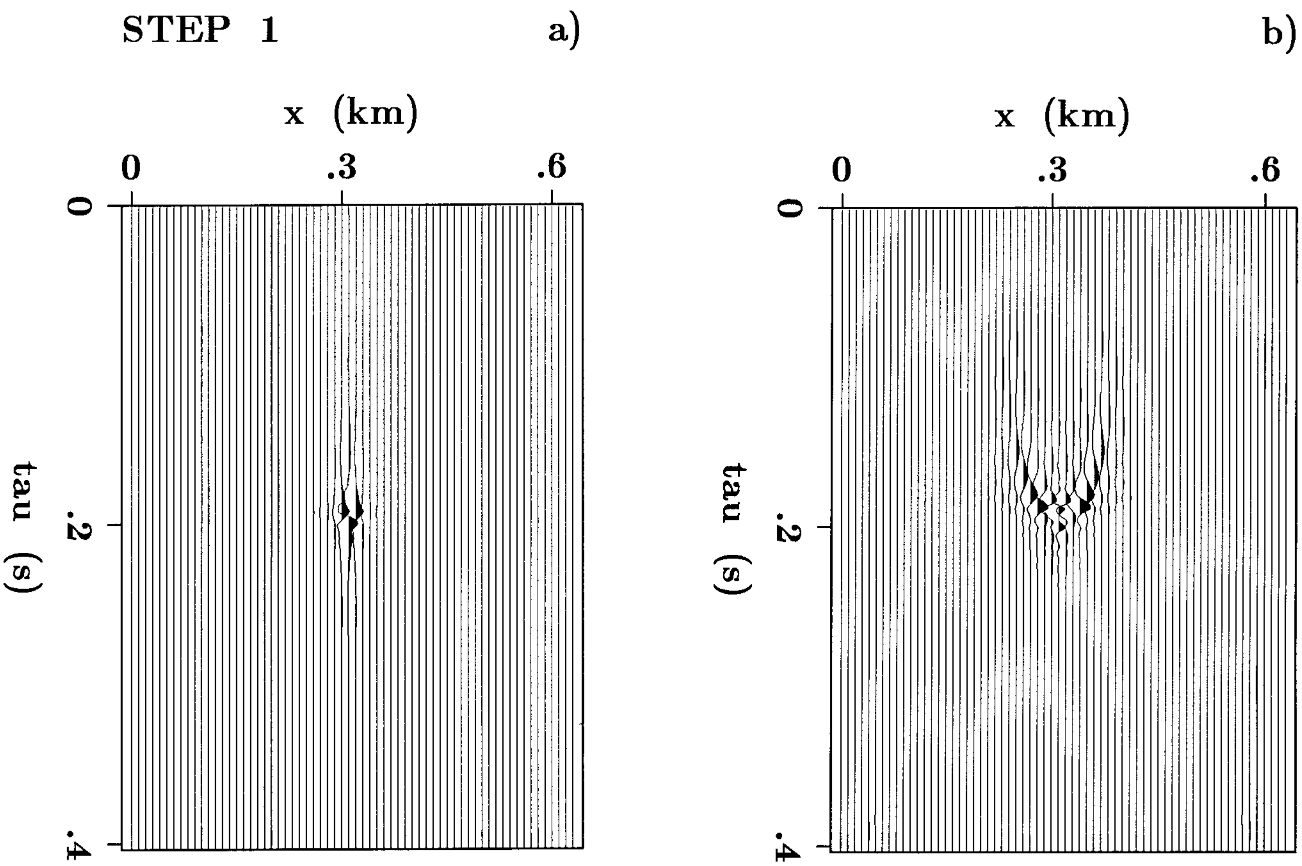

FIG. 5. Step 1 of the estimation procedure: we apply the gradient operator to the images of figure 4: the data are clipped above some level that we have set to 0.2 in this example. Figure a shows the small residual wavelet: $v_\epsilon = .10$ km/s, figure b the large residual wavelet with $v_\epsilon = .45$ km/s.

velocity perturbations are presented.

We see that for $v_\epsilon = 0.1$ km/s we get a sharp positive peak in the estimate around $\tau = 0.2$ s, the pseudo-depth of the input spike, whereas for $v_\epsilon = .45$ km/s the peak becomes more dispersed. Also, the amplitudes of the estimates are weaker in the latter case.

To get one value for the velocity perturbation, we sum the estimates over the τ-axis; we will call this value "step" as it will hopefully tell us how to "walk" in our search algorithm.

We now examine the behavior of the step for a range of residual velocities (see figure 8a). Figure 8b is a detailed picture of the estimate for residual velocities in the 10 %-accuracy region. We see that for this region the estimate is linear with velocity perturbation as predicted by the theory. Outside the region, the estimate gets smaller for larger velocity perturbations; there is less correlation between $m_{grad}(x,\tau)$ and $m_{diff}(x,\tau)$, because our first order approximation breaks

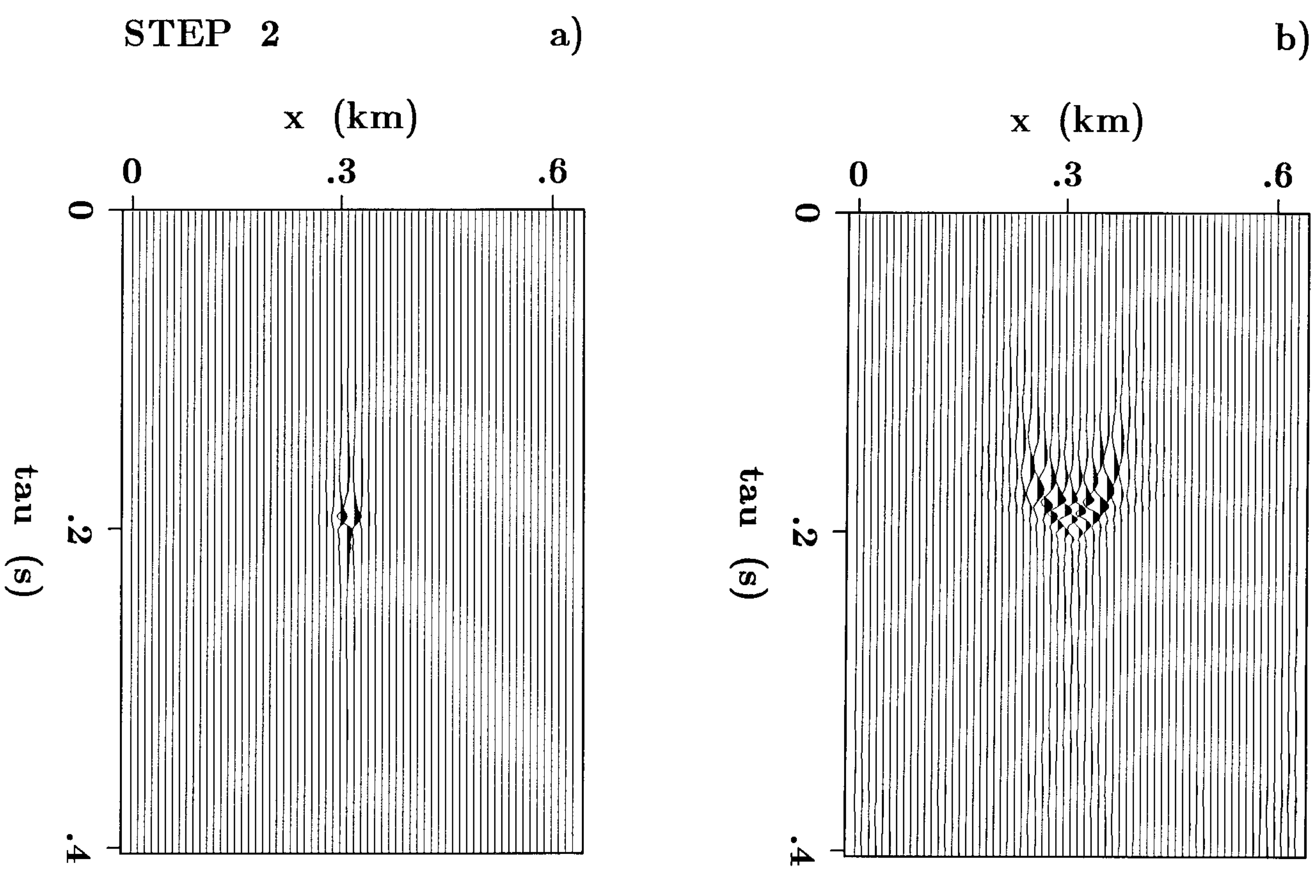

FIG. 6. Step 2 of the estimation procedure: the differential operator is applied to the images. Again, figure a displays $v_\epsilon = .10$ km/s, figure b $v_\epsilon = .45$ km/s.

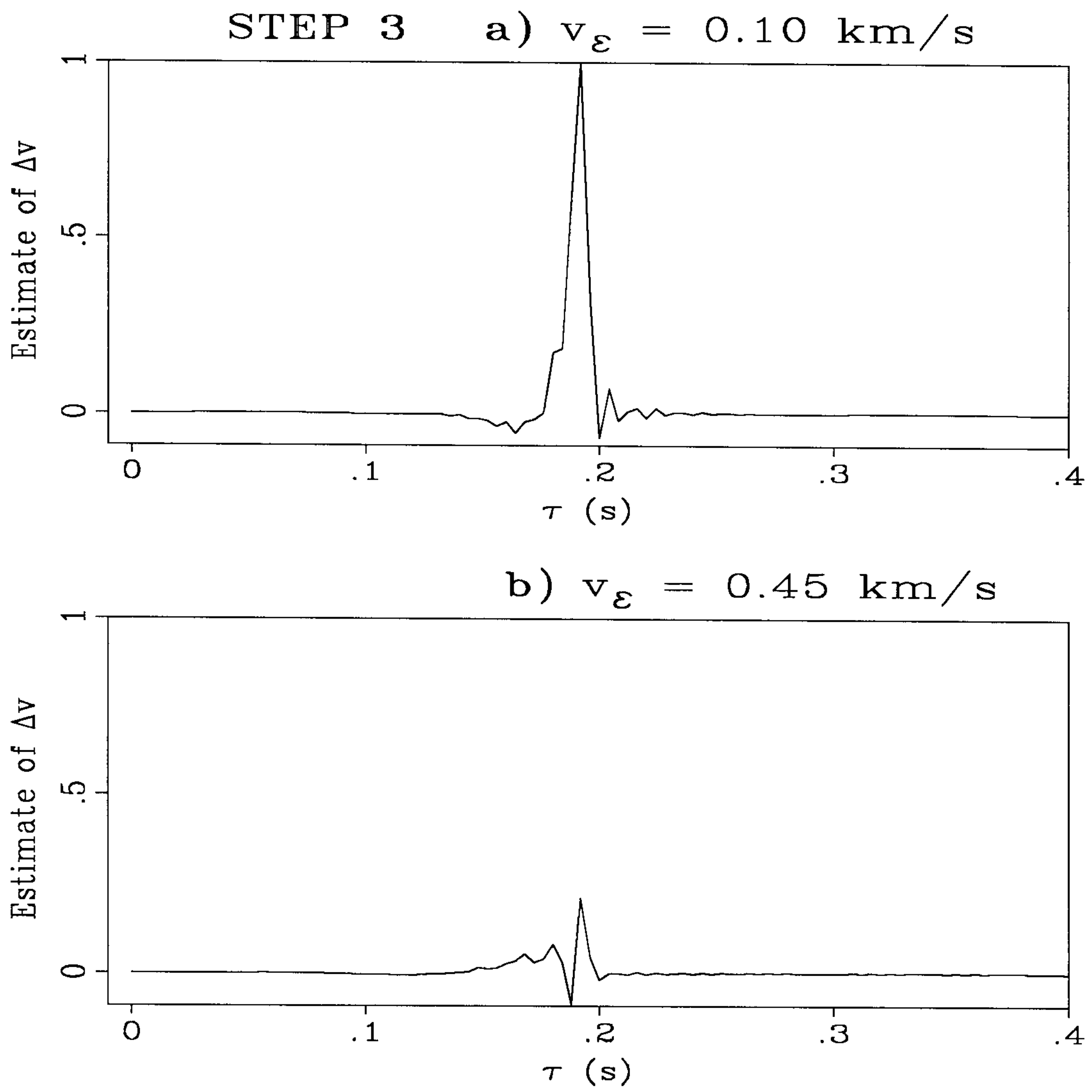

FIG. 7. Step 3: we take the dot product over x of the sections in figures 5 and 6, resulting in estimates of the velocity perturbation as a function of pseudo-depth for the two images of figure 4 (v_ϵ is 0.10 km/s in figure a, 0.45 km/s in figure b). The amplitudes of the estimates have been normalized to 1.

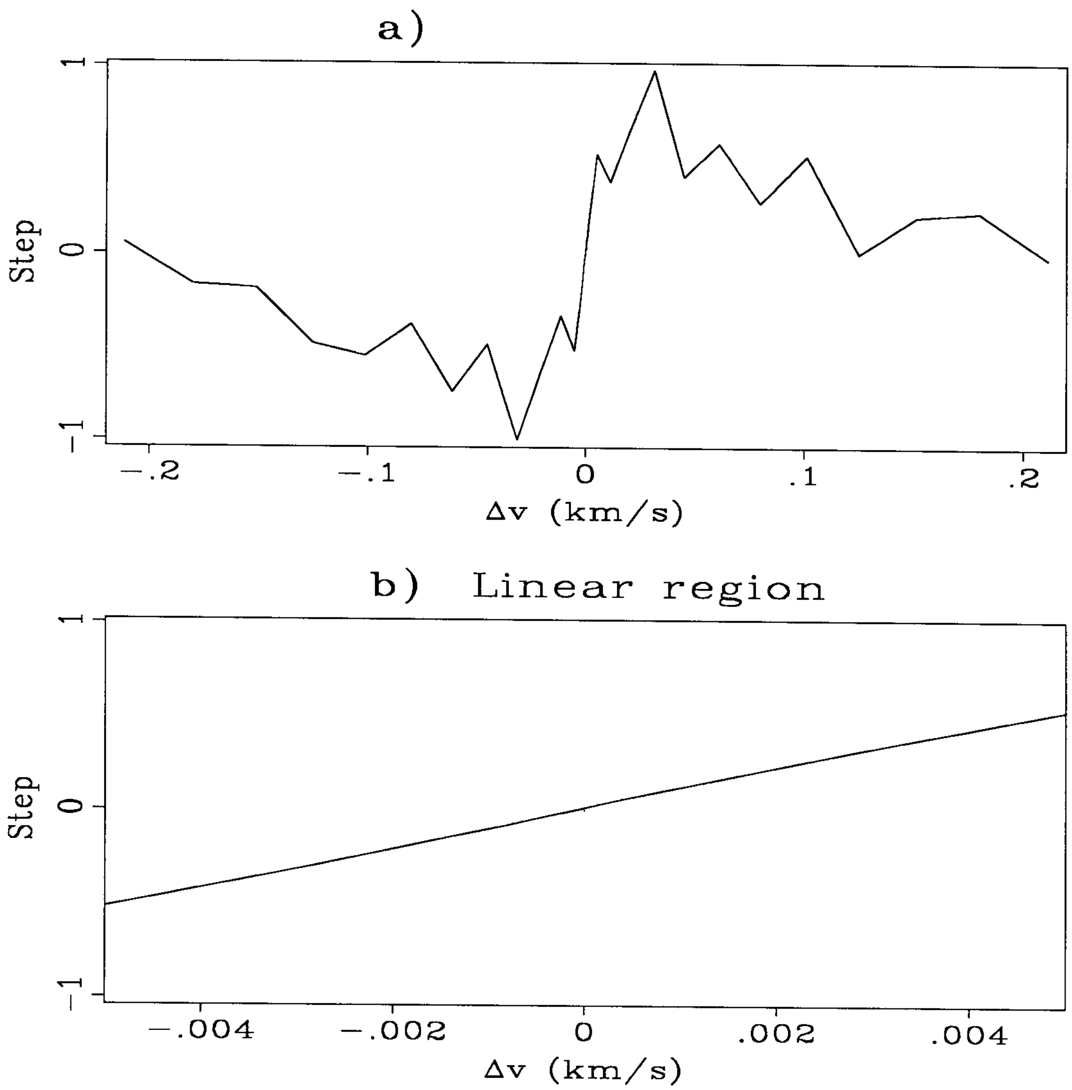

FIG. 8. Step as a function of the velocity perturbation (the difference between true and migration velocity). Figure b displays the linear region around $\Delta v = 0$ in detail. The clip value was 0.2. The amplitude of the step is normalized to 1.

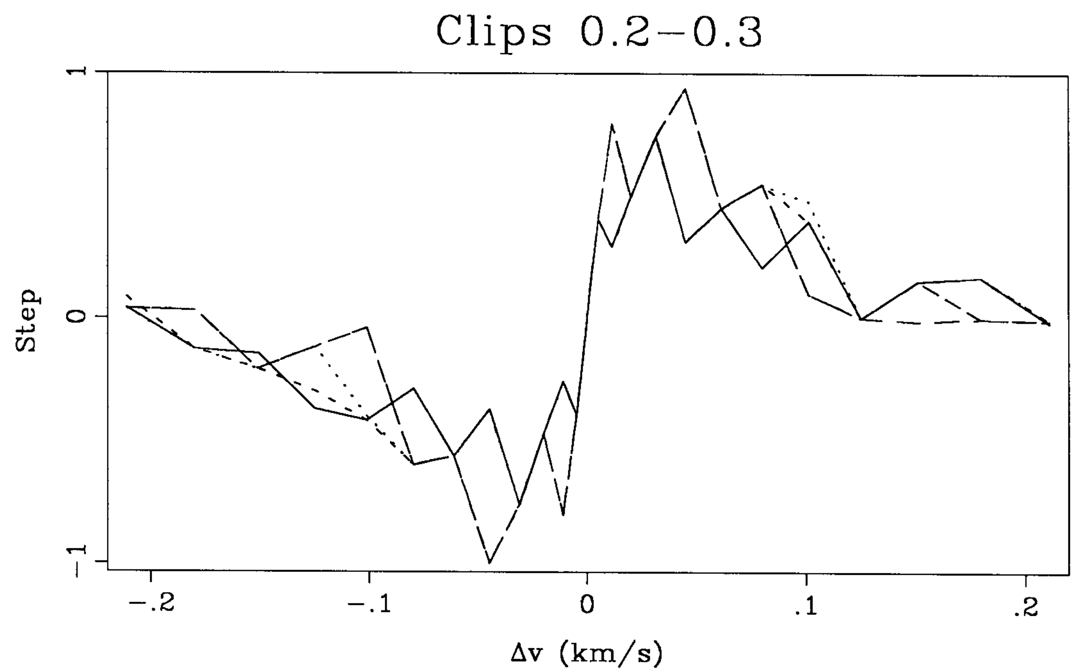

FIG. 9. Step function for clips 0.200, 0.225, 0.250, 0.275, and 0.300.

down. However, an important observation is that the *sign* of the estimate is still correct and this makes it possible to use the method in an iterative scheme.

Finally, we test the influence of the clip on the estimate. Figure 9 displays the estimate for several velocities and clips. In the linear region, the clip does not change the estimate much, whereas in the nonlinear region there is more variation with the clip. Again we notice that the sign of the estimate is correct for all clips (except for the very large velocity perturbations).

CONCLUSION

The described method enables us to determine residual velocities, even for a larger range of velocities than the one for which it originally was designed. The example we showed was useful as an illustration of the estimation procedure. Now the method has to be applied to more realistic cases than the one-spike model and it has to be incorporated in an optimization scheme that focuses the image automatically.

ACKNOWLEDGMENT

One of us (JvT) would like to thank Shell Internationale Petroleum Maatschappij for financial contributions.

REFERENCES

Dellinger, J., and Mora, P., 1986, Accurate finite difference operators by inversion: this report.

De Vries, D., and Berkhout, A.J., 1984, Velocity analysis based on minimum entropy: Geophysics, **49**, 2132–2142.

Godfrey, R.J., 1979, A stochastic model for seismogram analysis: PhD. thesis, SEP–17.

Harlan, W.S., Claerbout, J.F., and Rocca, F., 1984, Signal/noise separation and velocity estimation: Geophysics, **49**, 1869–1880.

Kostov, C., and Rocca, F., 1986, Estimation of residual wavelets: this report.

Mehta, S., 1977, Concurrent migration and velocity estimation in a random, non-gaussian earth: SEP report, **11**, 61–76.

Rocca, F., and Salvador, L., 1982, Residual migration: presented at the 52nd Annual International SEG meeting, October, Dallas.

Rothman, D.H., Levin, S.A., and Rocca, F., 1985, Residual migration: applications and limitations: Geophysics, **50**, 110–126.

Walden, A.T., and Hosken, J.W., 1985, The nature of the nongaussianity of primary reflection coefficients and its significance in deconvolution: presented at the 47th meeting of the EAEG, June, Budapest.

APPENDIX: CONDITIONAL MEAN

Kostov and Rocca (1986) describe a theory to estimate the wavelet $\underline{a}$ for the following convolutional model:

$$\underline{y} = (\underline{\delta} + \underline{a}) \ast \underline{x} = \underline{x} + \underline{a} \ast \underline{x} \tag{A1}$$

We will follow the same line of reasoning as they do to derive a formula for the estimate of $\underline{a}$, but will only use first order approximations. Furthermore, for residual modeling the wavelet $\underline{a}$ is determined by only one unknown Δv and we have to deal with an imaging step:

$$\underline{m}(\omega) = \int \left(\underline{\delta} + \Delta v \; \underline{b}(\omega,\tau)\right) \; * \; \underline{r}(\tau) \; \exp(-i\omega\tau) \; d\tau.$$

$$= \underline{r}(\omega) + \Delta v \int \underline{b}(\omega,\tau) \; * \; \underline{r}(\tau) \; \exp(-i\omega\tau) \; d\tau. \quad \text{(A2)}$$

This is the same equation as equation (7), where we have written the x-dependence in vector notation (e.g. $\underline{m}(\omega) = m(x,\omega)$). Likewise, we can express $\underline{r}$ in terms of $\underline{m}$ (residual migration):

$$\underline{r}(\tau) = \int \left(\underline{\delta} - \Delta v \; \underline{b}(\omega,\tau)\right) \; * \; \underline{m}(\omega) \; \exp(i\omega\tau) \; d\omega$$

$$= \underline{m}(\tau) - \Delta v \int \underline{b}(\omega,\tau) \; * \; \underline{m}(\omega) \; \exp(i\omega\tau) \; d\omega. \quad \text{(A3)}$$

Equation (A3) can be derived by approximating the dispersion relation in the same way as for residual modeling (equation (5)). To simplify equations, we substitute q for Δv and $\underline{w}_1$ and $\underline{w}_2$ for the integrals in equations (A2) and (A3):

$$\underline{m} = \underline{r} + q\underline{w}_1; \quad \text{(A4)}$$

$$\underline{r} = \underline{m} - q\underline{w}_2. \quad \text{(A5)}$$

Note that the first expression has ω as pseudo-depth variable, whereas the second expression uses τ for pseudo-depth. This distinction has to be kept in mind but is not relevant in the following analysis: the wavelets under consideration depend on x; pseudo-depth is an independent variable.

The conditional mean estimate of q is:

$$\hat{q} = \int q \; p_{\underline{m}}(q|\underline{m}) \; dq, \quad \text{(A6)}$$

where $p_{\underline{m}}(q|\underline{m})$ is the probability density function (pdf) of q, satisfying:

$$p_{\underline{m}}(q|\underline{m}) = \frac{p_{\underline{m}}(\underline{m}|q) \; p_q(q)}{p_{\underline{m}}(\underline{m})}. \quad \text{(A7)}$$

To evaluate this expression, we first use the following theorem for $p_{\underline{m}}(\underline{m})$:

$$p_{\underline{m}}(\underline{m}) = \int p_{\underline{m}}(\underline{m}|q) \; p_q(q) \; dq \quad \text{(A8)}$$

and then approximate $p_{\underline{m}}(\underline{m}|q)$ to first order in q using (A5):

$$p_{\underline{m}}(\underline{m}|q) = p_{\underline{r}}(\underline{m}) \; - \; q \; p'_{\underline{r}}(\underline{m}) \; \cdot \; \underline{w}_2 \quad \text{(A9)}$$

We substitute expressions (A7)–(A9) in equation (A6):

$$\hat{q} = \frac{-\overline{q^2}\; p'_{\underline{r}}(\underline{m}) \;\cdot\; \underline{w}_2}{p_{\underline{r}}(\underline{m})} \tag{A10}$$

$$= \; -\overline{q^2}\; \gamma(\underline{m}) \;\cdot\; \underline{w}_2, \tag{A11}$$

where we have used:

$$1 = \int p_q(q)\; dq; \tag{A12}$$

$$\overline{q} = \int q\; p_q(q)\; dq = 0; \tag{A13}$$

$$\overline{q^2} = \int q^2\; p_q(q)\; dq; \tag{A14}$$

$$\gamma(\underline{m}) = \frac{p'_{\underline{r}}(\underline{m})}{p_{\underline{r}}(\underline{m})}. \tag{A15}$$

The first order approximation of the pdf is only valid for small $\overline{q^2}$; for very large values of the variance we have to use a gain factor as in Kostov and Rocca (1986).

Godfrey (1979) derived an expression for the behavior of the gradient function γ (see figure 1) in the case where the pdf for $\underline{r}$ is a Gaussian mixture. In our convolutional model $\underline{r}$ is the reflectivity sequence and the use of a Gaussian mixture for the pdf of the reflectivities is justified by Walden and Hosken (1985).

We now change back to our original notation:

$$\widehat{\Delta v}(\tau) \;=\; \overline{\Delta v^2}\; \gamma\big(\underline{m}(\tau)\big) \;\cdot\; \int -\big(\underline{b}(\omega,\tau) * \underline{m}(\tau)\big)\; \exp(i\omega\tau)\; d\omega. \tag{A16}$$

Researchers have already cast much darkness on the subject, and if they continue their investigations, we shall soon know nothing at all about it.

MARK TWAIN.